

---

# Mathematical modelling of morphogenesis in fungi: spatial organization of the gravitropic response in the mushroom stem of *Coprinus cinereus*

---

A. MEŠKAUSKAS, DAVID MOORE\* AND LILYANN NOVAK FRAZER

*School of Biological Sciences, The University of Manchester, Manchester M13 9PT, UK*

*(Received 10 February 1998; accepted 20 May 1998)*

## SUMMARY

The purpose of this work was to establish how the distribution of local curvatures changed during the mushroom stem gravitropic reaction and to suggest a suitable mathematical model based on these new data.

The gravitropic bending of base- and apex-pinned *Coprinus cinereus* (Fries) S. F. Gray stems was recorded on videotapes. The images were captured from the tapes after each 10 min, rotated by 45° and transformed into tables of changing co-ordinates of points for each stem. The non-linear regression of these points was performed using Legendre polynomials. From the resulting equations the patterns of changing local curvature for 50 subsections per stem during 400 min of gravitropic reaction were calculated.

It was observed that base-pinned stems first bent from the apex, but later the curvature of this part decreased, and in the late stages the apex became nearly completely straight again. Subsections, located about one third of stem length from the base determined the main part of the final curvature. The free basal part of the apex-pinned stems bent upward and after a certain bending time also began to straighten. However, this process started significantly later and was weaker. Bending of the subsections close to the pinned apex did not stop when they reached the vertical position, and the final angle of gravitropic curvature could exceed 180°.

Plotting various functions of local bending speed and its derivatives against each other and against local angle indicated that, if the hypothetical signal about reorientation arises in the apex, its propagation towards the base did not follow simple wave or simple diffusion laws. The importance of the local angle of all subsections both for signal origin and transmission was established and a signal transmission equation, involving local angle of each subsection, was derived. After creating a suitable program this partial differential equation was solved numerically. The generated shapes of the bending stem coincided in high degree with experimentally observed images.

**Key words:** Mathematical models, computer simulation, signal transmission, *Coprinus cinereus* (Fries) S. F. Gray, gravitropism.

## INTRODUCTION

Computational models have been developed which describe successfully and simulate the morphology, growth and development of plants (Korn, 1993; Pankhurst, 1994; Prusinkiewicz & Lindenmeyer, 1996). We have adopted an approach which uses the gravitropic reactions of mushroom fruit bodies as an experimental system to study control of morphogenesis in fungi by defining the kinetics and cellular morphometrics of the tropic bending response. The rationale of this strategy is that altered orientation to

the gravity vector provides a non-invasive initiator of a defined morphogenetic change which is easily replicated and open to precise experimental control. Combination of a variety of microscopic observation techniques, coupled with video observation and image analysis permits detailed kinetic descriptions to be assembled (Moore *et al.*, 1996; Greening, Sánchez & Moore, 1997). These quantitative observations provide the basis for development of mathematical models aimed at simulating the tropic response.

Computer-based video analysis of organ shape has been used to analyse the pattern of growth rates and local angles for *Arabidopsis thaliana* (Evans & Ishikawa, 1997), and in this paper we apply a similar

\* To whom correspondence should be addressed.  
E-mail: david.moore@man.ac.uk

method to the mushroom stem with the particular aim of establishing how the distribution of local curvature changes during morphogenic bending so that mathematical modelling can be used to examine signal transmission. From a variety of known transmission equations (Whitham, 1977), the concept describing a 'wave with decrement' (that is, reduced amplitude in successive waves) has been used most commonly to represent signal transmission during the gravitropic reaction. There is no direct evidence for the applicability of this equation in fungal gravitropism. It is known that the point of inflection of the stem of *C. cinereus* moves from the apex to the base with decreasing speed (Kher *et al.*, 1992). However, this could mean that the signal also moves with decreasing speed, which is not a characteristic of wave transmission. Another important assumption of many models of plant gravitropism is that signal perception takes place exclusively in the apex, from which it is later transmitted in the basipetal direction. However, it is known that *C. cinereus* stems are able to respond gravitropically even after removal of up to 60% of their apical parts (Greening, Holden & Moore, 1993). This could indicate that the hyphal system of a mushroom stem has much greater autonomy than, for example, plant coleoptiles which lose their ability to react gravitropically after decapitation, until the apex regenerates (Went, 1928).

Stočkus & Moore (1996) succeeded in simulating the gravitropic change in apex angle of mushroom stems using imitational modelling. The assumption of their basic scheme, which was derived from those of Rawitscher (1932) and Merkys, Laurinavičius & Jaročius (1972), was that changes of apex angle occurred as a result of four consecutive stages – the physical change which occurs when the subject is disoriented, conversion of the physical change into a physiological change, transmission of the physiological signal to the competent tissue and, finally, the growth response in which differential regulation of growth generates the change in apex angle. A combined equation was established which could generate simulated kinetics which imitated the reaction of mushroom stems quite well.

The imitational models of Stočkus & Moore (1996) dealt with change in apex angle only. The bending process forming the apex angle was reduced to a 'mathematical point'. It is evident from the observations which have been made (Kher *et al.*, 1992; Moore *et al.* 1994), that distribution of bending rates in mushroom stems is rather complex. There are regions, that, after reaching a certain angle, start to straighten. Almost 90% of the initial curvature is compensated by this process so it cannot be ignored. Consequently, a more realistic model of the mushroom stem gravitropic reaction must be at least 1 + 1-dimensional, describing the bending process not only in time but also in space.

One of the first such models for plants was created by Johnson & Israelson (1968). They supposed that local bending rate depends on a signal which is generated in the tip and then moves in a basipetal direction at constant speed (in effect, as a wave moving away from the apex). The ability of different subsections to respond to this signal, called a competence function, was found empirically. Later, the model was modified (Johnson, 1971; Brown & Chapman, 1977), but the equation parameter defining signal transmission remained the same in the different treatments. Barlow *et al.* (1991) also assumed the same transmission law in their model. Stočkus (1994) also proposed a model which assumed that a gravitropic signal moved in a basipetal direction as a wave, weakening as it progressed. This model was applied to *C. cinereus* by Stočkus & Moore (1996). However, restricting attention to change in tip angle was a significant limitation. Fungal gravitropic kinetics is more dependent on *how* curvature is realised along the stem and a computational model able to mimic that would be a much more valuable morphogenetic paradigm.

## MATERIALS AND METHODS

### *Experimental material*

The vegetative dikaryon of *Coprinus cinereus* (Fries) S. F. Gray was cultured on complete medium (Moore & Pukkila, 1985) in 9-cm Petri dishes in the dark at 37 °C for 3–4 d. Fruiting bodies were obtained by inoculating the dikaryon onto sterilized horse dung in crystallizing dishes, incubating at 37 °C for 3–4 d in the dark and then transferring the dung cultures to a 26–28 °C incubator with a 16 h light/8 h dark illumination cycle (white fluorescent lights, average illuminance 800 lx). The length of the stems used at the start of observation was 40–48 mm. The standard assay of *C. cinereus* gravitropism involved removal of the cap followed by continuous video recording of the stem secured on a horizontal platform, housed in a humidity chamber at room temperature. Video records give no evidence for rotation of the fruit body stem during either vertical growth or tropic bending. Each chamber typically contained one base-pinned, one apex-pinned and one vertical stem. The data from 14 apex-pinned, 14 vertical and 13 base-pinned stems were collected for analysis.

### *Image capture, analysis and mathematical model fitting*

The images were captured from videotapes using Screen Machine Camera® v. 1.1 peripherals and software at a resolution of 736 × 560 points per image (c. 10 points mm<sup>-1</sup>). Images were captured every 10 min up to 400 min, producing 41 images for each

stem. Images were manipulated using Image Assistant® v. 1.10. Graphic images were digitized into  $x$ - $y$  coordinates using UnGraph® v. 3.0. For mathematical analysis the digitized stem images were divided into 50 subsections. Images were rotated before regression analysis. Regressions and calculation of curvatures and local angles were performed using Maple® V, v. 4.00b. Subsequent analysis was done with Mathcad® v. 6.0, using function libraries written or generated in Borland® C++ v. 5.02. The final model was written in Borland Pascal v. 7.0 using object-oriented programming.

## RESULTS AND DISCUSSION

### The measured parameters

The measured parameters which were most informative in describing the bending process in the stem during gravitropic reaction were the local angle  $\alpha_L$  and the local curvature  $C_L$ .

The angle by which a short subsection of the mushroom stem (in our analyses 'short' = 2% of total length) is disoriented from the horizontal was taken to be the local angle ( $\alpha_L$ ), mathematically defined as the tangent of the inclination. Without prejudgement of mechanism, signal perception can be described as a function of  $\alpha_L$  at any point along the stem which is disoriented from the vertical. However, the local angle at any point does not reflect the bending process developing *at* that specific point because bending is a property of segments adjacent to that for which  $\alpha_L$  is measured. Hence, it is necessary to establish a parameter which reflects reliably the bending process in any particular segment independently of adjacent segments. Such a parameter is the mathematical description of curvature (Borwein, Watters & Borowski, 1997).

Mathematically, curvature reflects the rate of change of the local angle through the curve. According to Piskunov (1969), curvature is the rate of change of inclination of the tangent to a curve relative to the length of arc, and is measured in units of degrees per unit length. This mathematical definition of curvature has been used in work with plants by Silk & Erichson (1979) and Silk (1989), but the definition of curvature used by Evans & Ishikawa (1997) is more related to local angle.

It was initially assumed that subsection curvature reflected the apex angle, i.e. the angle to the horizontal that the apex would express if all subsections had the same curvature as this subsection. Mathematically, then, both  $\alpha_L$  and  $C_L$  are functions of any point of the curve. In our case they can depend on point distance from the stem base ( $\lambda$ ) and on time. The meaning of these parameters is illustrated in Figure 1.

The stem continues to elongate as it bends and there is some physiological evidence that these two

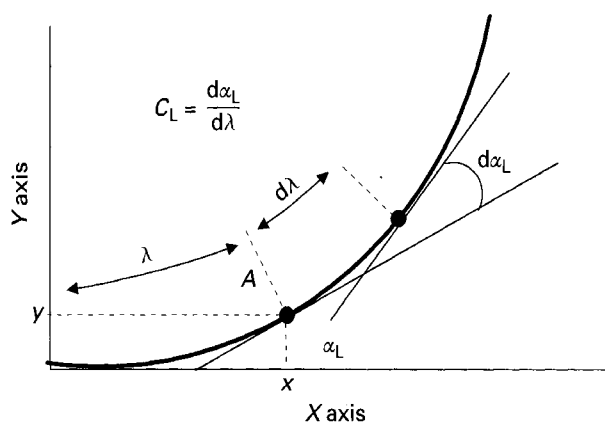


**Figure 1.** Definition of the local angle ( $\alpha_L$ ), curvature ( $C_L$ ), distance from the base ( $\lambda$ ) and point  $x$  and  $y$  co-ordinates. Curvature is a ratio, calculated using the formula shown in the text, true as  $d\lambda$  tends to zero.  $d\alpha_L$  is mathematically defined as the angle of contingence. All parameters are illustrated for point  $A$ .

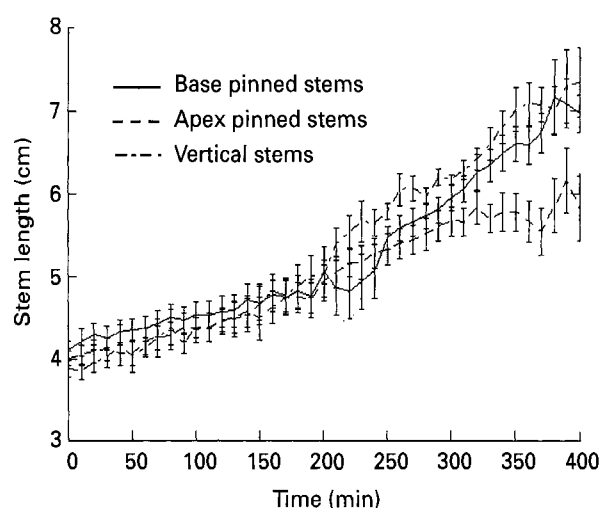


**Figure 2.** Influence of reorientation into the horizontal position and further gravitropic reaction on the growth of *Coprinus cinereus* stems. The error bars represent SD of the mean.

growth processes are different (Novak Frazer & Moore, 1993; Greening *et al.*, 1997). Stem length was calculated from the data points generated by UnGraph during digitization (Fig. 2). Reorientation of base-pinned stems to the horizontal position and the subsequent gravitropic response did not affect elongation of the stems in the first 200 min as the apex angle reached the vertical. In apex-pinned stems, however, in which the stem continued to bend past the vertical, there was a statistically significant reduction in elongation compared with vertical (that is, undisturbed) and base-pinned stems. The cause of this is unknown. Pinning the apex may cause damage which reduces ability of the tissue to generate hormonal growth factors. On the other hand the range of hormones produced may depend on the orientation of the apex. In all other analyses reported here the stems from different treatments were normalized to a standard length for ease of analysis.

**Table 1.** Illustration of the technique for finding local curvature distribution in a real *C. cinereus* stem using 2nd degree polynomial regression (calculations performed by Maple V.)

Description	General equation	Equation if stem shape is approximated by parabola	Equation for a real <i>C. cinereus</i> stem 240 min after reorientation to the horizontal
Stem shape as y co-ordinate function from x co-ordinate	$y(x)$	$b_0 + b_1 x + b_2 x^2$	$0.0100662187 - 1.626461944 x + 1.522987778 x^2$ in interval [0...0.8] (rotated by 45°)
Local curvature as a function of the x co-ordinate	$\frac{y''}{(1+(y')^2)^{\frac{3}{2}}}$	$\frac{2}{(1+(b_1+2x)^2)^{\frac{3}{2}}}$	$\frac{3.045975556}{(1+(-1.626461944+3.045975556 x)^2)^{\frac{3}{2}}}$
Distance from the base to the point with co-ordinate x	$\int_0^x \sqrt{1+y'^2} dx$	$\int_0^x \sqrt{1+b_1^2+4b_1 x+4x^2} dx$	$\int_0^x \sqrt{1+(-1.626461944+3.045975556 x)^2} dx$

*Calculating the curvature and local angle from digitized data*

If the stem shape is expressed by the explicit equation  $Y = y(X)$ , where  $X$  and  $Y$  are co-ordinates, local angle and curvature can be found for each point using:

$$\alpha_x(x) = \text{arc tg}(y'(x))$$

$$C_x = \frac{y''(x)}{(1+y'(x)^2)^{\frac{3}{2}}}, \tag{1}$$

where  $y'$  and  $y''$  are the first and second  $y$  derivatives on  $x$  respectively.

If stem shape is described by a 3rd order polynomial regression of the form  $y(x) = b_0 + b_1 x + b_2 x^2 + b_3 x^3$ , where  $y(x)$  is the function describing stem shape and  $b_0 \dots b_3$  are coefficients determined from the digitized data, the first and second derivatives are:

$$y'(x) = \frac{d}{dx} y(x) \rightarrow b_1 + 2 b_2 x + 3 b_3 x^2$$

$$y''(x) = \frac{d^2}{dx^2} y(x) \rightarrow 2 b_2 + 6 b_3 x.$$

Hence the curvature is:

$$C_x(x) = \frac{y''(x)}{[1+(y'(x))^2]^{\frac{3}{2}}} \rightarrow \frac{2 b_2 + 6 b_3 x}{[1+(b_1+2 b_2 x+3 b_3 x^2)]^{\frac{3}{2}}}$$

To find  $\lambda$  from  $x$ , we can use the formula for calculating the curve arc length that leads to the integral:

$$\lambda(x) = \int_0^x \sqrt{1+y'(x)^2} dx \tag{2}$$

It is possible to plot  $C_x(x)$  and  $\alpha_x(x)$  against  $\lambda(x)$ , calculating  $\lambda$  from  $x$  using (2), and changing  $x$  from 0 to the value  $x_{\text{max}}$  such that  $\lambda(x_{\text{max}})$  is equal to stem length. This allows  $\alpha_l$  and  $C_l$  to be obtained rapidly,

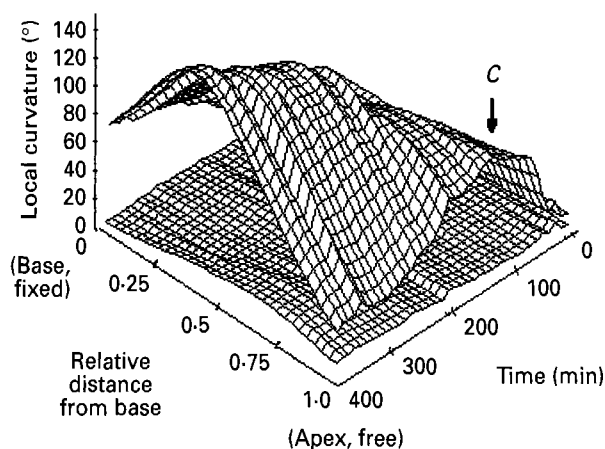


**Figure 3.** Surfaces generated by Maple V which show how local curvature changes during the gravitropic reaction of base-pinned *C. cinereus* stems. Distance from the base is given in arbitrary units of stem length. Upper surface represents average curvature, in angular degrees. Lower surface is standard mean deviation, calculated separately for each point.  $C$  indicates the beginning of the compensation process (curvature near the apex starts to reduce).

but restricts further analysis. An alternative is to try to solve eqn (2) for  $x$ . As a rule, it is not easy to get a unique solution, but it is possible to use numeric methods.

For each *Coprinus* stem analysed, changes in local angle and local curvature in all 50 subsections through time during the gravitropic reaction were calculated. Then, from these data, the progress of gravitropic bending as it developed in an 'average' stem was calculated. An example of the application of these steps to one *Coprinus* stem is illustrated in Table 1. Application of the steps described in Table 1 produced a separate description of how curvature changed with time for each stem used for analysis. Values of curvature of the same segment, at the same time, but in *different* stems, were then combined to calculate means and SD. Illustrations of data surfaces (e.g. Fig. 3) include a surface describing the SD for each point of the surface. In time- and space-telescoped projections (e.g. Fig. 4) a single error bar

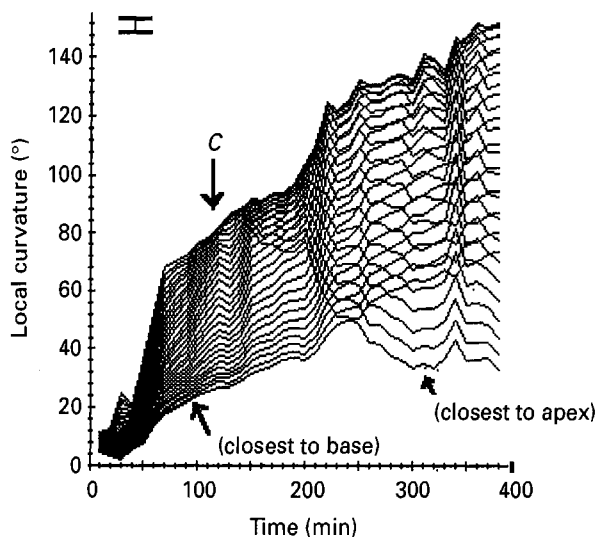


**Figure 4.** The distribution of local curvature over the length of the stem for base-pinned *C. cinereus* stems. Each curve represents the changing curvature of a different stem subsection. Error bar represents maximal SD. See Figure 3 for time scale and more exact standard deviation estimation. *C* shows the start of the curvature compensation process (apical subsections start to straighten).

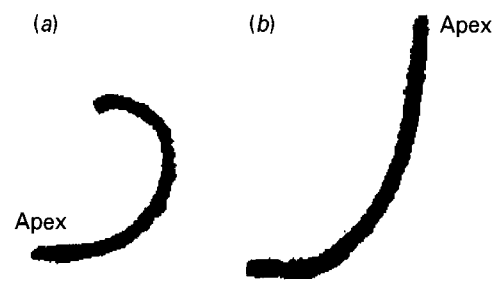
(maximal SD of the mean, both for vertical and horizontal co-ordinates) is shown because of the large number of data points involved.

*Local curvature as a two-parameter function of position and time in C. cinereus base- and apex-pinned stems*

Since subsection curvature depends on subsection position in the stem and also changes with time, its change during the gravitropic response can be presented as a surface with horizontal co-ordinates representing time and distance from the base. This surface, averaged for 13 base-pinned stems, is illustrated in Figure 3.

Figure 3 shows that after reorientation into the horizontal position, upward curvature of the stem first starts close to the apex. As time progresses, the curvature spreads towards the base with decreasing speed. Finally, the maximum curvature practically stops in a position approx. 0.3 of stem length from the base, by which time the apex angle has reached 90°.

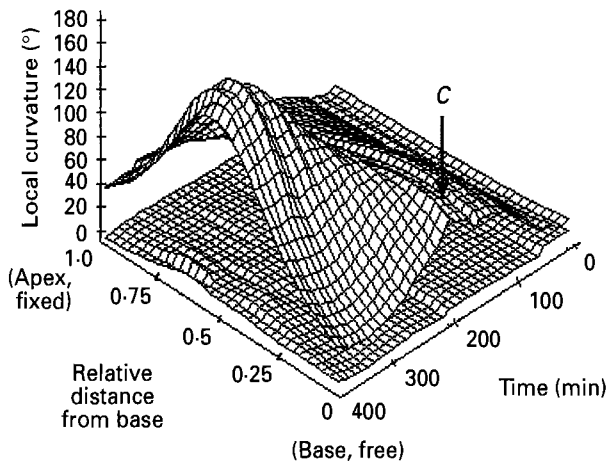
Barlow & Rathfelder (1985), measuring the distribution of elemental growing rates along bending maize root, observed the bell-shape distribution, but concluded, that the peak of the curvature remained stationary during this gravitropic reaction. Computer-generated root images, based on this assumption, were considered to be realistic (Barlow, Brain & Adam, 1989). The peak curvature of the plumule hook of *Pharbitis nil* also remained at the same distance from the tip during hook maintenance (Silk, 1989). Basipetal movement of the point of maximum curvature may be an important difference between the gravitropic mechanics of mushrooms and plants.



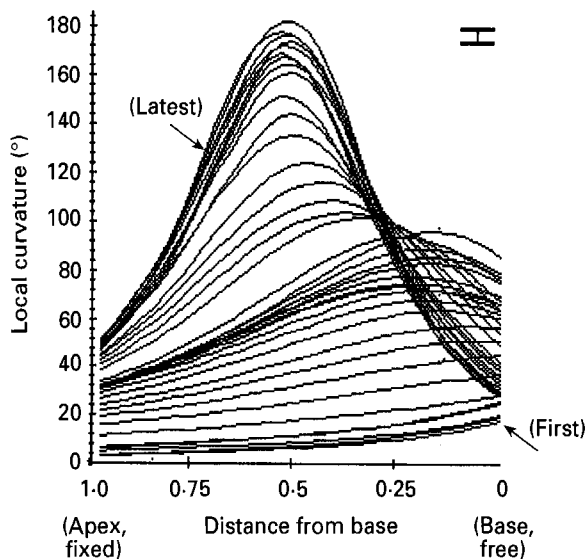
**Figure 5.** The image of apex-pinned (a) and base-pinned (b) *C. cinereus* stems 400 min after reorientation to the horizontal position.

Figure 3 also shows that curvature of the most apical subsections starts to decrease after *c.* 100 min (indicated by arrow *C*). This process starts well before the apex reaches the vertical position and is called curvature compensation (Kher *et al.*, 1992; Moore *et al.*, 1994). The regularities of curvature compensation are most clearly seen in Figure 4 which is the projection of the response surface into the time plane and clearly indicates that curvature compensation first begins close to the apex. Thus, despite the fact that this part also reacts gravitropically the most rapidly, the major part of its tropic curvature is later cancelled by the compensation process. Intermediate subsections closer to the base exhibit weaker compensation; their gravitropic bending is significant and its persistence determines the final angle of the apex. The most basal subsections have no detectable compensation and show only a weak gravitropic reaction. Thus, acting together, tropic bending and curvature compensation processes form the bell-shaped distribution of local curvature, the peak of which first coincides with the apex, then moves towards the base with decreasing speed.

The question arises of how much these processes depend on the polarity of the stem. In both *C. cinereus* (Kher *et al.*, 1992) and *Flammulina velutipes* (Monzer *et al.*, 1994) it is known that when the apex is fixed to the horizontal support the stem does not stop bending when the base reaches a vertical position. Instead, bending continues, and the total angle of gravitropic bending in later stages can exceed 180° (Fig. 5). Applying the same approach as used previously, the surface describing changes in local curvature with time and position, averaged for 14 apex-pinned stems, appears as in Figure 6. Compared with the base-pinned counterpart (Fig. 3), it is more difficult to say when the bending process begins. Figure 7 (the time-telescoped projection) suggests that the stem does not bend at all in the first 30 min (the first three curves are very close to each other). However, Figure 6 is strikingly similar to Figure 3 and curvature was greater near the free base in the early stages, then the peak of curvature moved towards the apex with decreasing speed. In apex-pinned stems, movement of the peak curvature stopped much earlier, somewhere in the



**Figure 6.** Surfaces generated by Maple V which show how local curvature changes in apex-pinned *C. cinereus* stems. Distance from the base is given in arbitrary units of stem length. Upper surface represents average curvature, in angular degrees. Lower surface is standard mean deviation, calculated separately for each point. C shows the start of curvature compensation (curvature near the base starts to reduce).



**Figure 7.** The distribution of local curvature over the length of the stem for apex-pinned *C. cinereus* stems. Curves represent 10-min time intervals. Distance from the base is given in arbitrary units of stem length. Error bar represents maximal standard deviation. See Figure 6 for time scale and more exact standard deviation estimation.

middle of the stem, and then *increased* in magnitude, reaching values exceeding 180° (with base-pinned stems, maximum curvature did not exceed 140°). This high final value of the curvature maximum peak was the cause of the stem finally curling through 180°, as displayed in Figure 5.

The most unexpected feature emerging from Figure 6 is that the bending process of apex-pinned stems is accompanied by a degree of curvature compensation (arrow C in Fig. 6). Although the reduction of local curvature near the free end is weaker than it is in base-pinned stems, it is statistically significant. From Figure 8, which is the projection onto the time plane, it is evident that

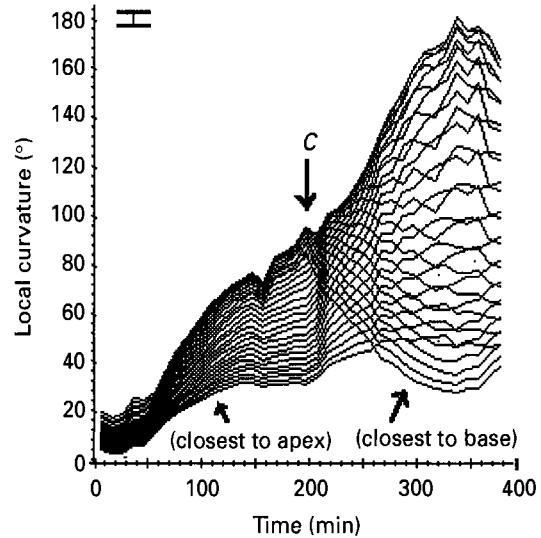


**Figure 8.** The distribution of local curvature over the length of the stem for apex-pinned *C. cinereus* stems. Each curve represents the changing curvature of a different stem subsection. Error bar represents maximal SD. See Figure 11 for time scale and more exact standard deviation estimation. C shows the start of the curvature compensation process (basal subsections start to straighten).

curvature compensation begins much later; approx. 200 min after reorientation in comparison with approx. 80 min for the normal gravitropic reaction. It is also evident that after approx. 340 min the curvature of subsections closest to the free end (= the stem base) starts to increase again. This was not observed with the base-pinned stems (Fig. 4).

Evidently, the way gravitropic curvature changes with time is different between apex-pinned and base-pinned stems. For base-pinned stems the peak curvature is located closer to the base and attains lower values, leading to a final apex angle close to the vertical. For apex-pinned stems, peak curvature is located near the middle of the stem and reaches high values, leading to the base bending well beyond the vertical. The compensation process for apex-pinned stems is significantly delayed and in very late stages of the gravitropic reaction it tends to reverse (possibly a consequence of the apex (futile) hunting for the vertical?). In both cases the peak of the local curvature distribution curve moves away from the end of the stem which is free to bend and towards the end which is pinned. One interpretation of these features would be that apex and base of the stem are both able to perceive the gravity vector and are the source of a wave of bending signal first and subsequently are the source of a wave of signalling which promotes curvature compensation. In other words the stem might be bipolar. However, it is also possible that the 'similarities' between base-pinned and apex-pinned stems are spurious. It is noticeable that in apex-pinned stems the curvature compensation occurs only after gravitropic curvature has rotated the basal regions past the vertical and back towards the horizontal. It might, therefore, be a secondary gravitropic response in tissues which have

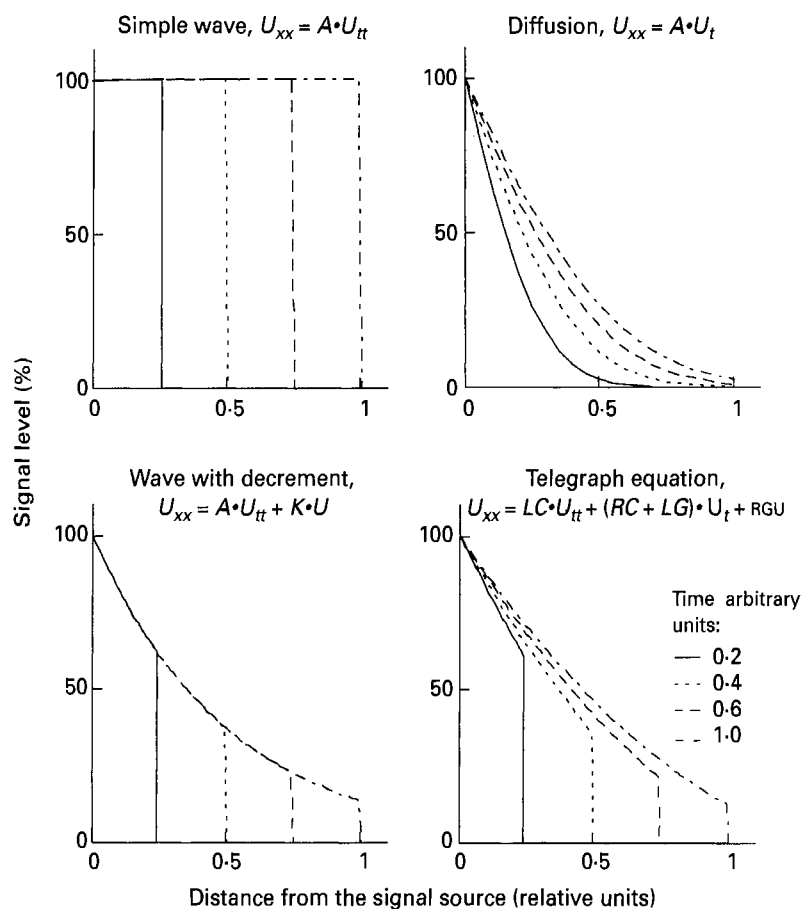


**Figure 9.** Schematics of the one-dimensional pattern of signal flow expected under different transmission processes: simple wave transmission (D'Alembert's principle), diffusion, wave with decrement and the telegraph equation.  $U$  = signal level;  $U_t$ ,  $U_{tt}$  = signal rate and acceleration;  $U_{xx}$  = second derivative of the signal relative to distance from source;  $A$  = parameter determining transmission rate;  $K$  = parameter determining signal decrement;  $R$ ,  $L$ ,  $C$  and  $G$  are parameters in the telegraph equation which determine signal transmission rate and influence its form. Sample curves were generated using Mathcad.

been rotated between  $90^\circ$  and  $180^\circ$  and so be of a different nature to that which occurs in stems which are base-pinned. Also, the progression of the peak of local curvature towards the apex in apparent contradiction to normal stem polarity might be an artefact. Since the basal regions of the stem are unable to bend, a continuous bending signal emanating from the apex fixed on the horizontal support could cause the curvature of the already bent parts of the stem to become increasingly emphasized with the inevitable result that the peak of local curvature will appear to move towards the apex even though the signal is emanating from the apex. These features are open to test using the computational model discussed below.

#### *Searching for a suitable signal transmission equation*

Many successful mathematical models of plant gravitropism are written as functions of bending velocity vs. tip angle or bending acceleration versus bending velocity and tip angle. Such models usually assume that after reorientation a particular 'signal' arises in a subsection and the bending velocity or acceleration is proportional to the level of this signal. Although, in biological terms, it is important to understand the exact nature of the signal, one of the

advantages of these models is that they do not need this information. The 'signal' can be incorporated as an abstract parameter which is proportional to the bending speed or acceleration.

The signal is often supposed to arise in the apex, reaching some target below the apex after a time delay of several min or tens of min. Using partial differential equations it is possible to write models which describe other circumstances. For example, the signal might arise through the whole length of the stem and response depends on distribution of a competence function. Alternatively, the signal might propagate in accordance with a particular physical law like diffusion or wave motion. To examine these possibilities for the gravitropic reaction of *C. cinereus* stems the signal was assumed to be proportional to the velocity of change in local curvature. In this case the signal intensity can be measured in  $\text{degrees s}^{-1} \text{m}^{-1}$ . If distance is measured as a proportion of the stem length, this unit changes to  $\text{degree s}^{-1}$ . Hence,

$$U = \frac{dC_L}{dt}, \quad (3)$$

where  $U$  is local bending velocity.

Bending rate and acceleration are first and second derivatives on time. It is also possible to get

derivatives on distance from the base ( $\lambda$ ). The first derivative is the curvature gradient. It is obvious that the bending rate gradient or bending acceleration gradient can also be calculated. The second derivative is the 'gradient of gradient'. Using this derivative, it is possible to test hypotheses that any observed 'signal' is spreading in accordance with the most frequently encountered transmission equations (Fig. 9).

Tests of the *Coprinus* data showed that neither diffusion, wave motion, nor the general telegraph equation could account for signal transmission in the *C. cinereus* stem during its gravitropic reaction. Their inability to account for signal transmission in the stem was taken to mean that the true signal transmission equation must include a parameter which changes during the progress of the gravitropic reaction. What changes most, of course, is the curvature, so an obvious possibility is that the behaviour of each subsection depends on the subsection local angle. This hypothesis assumes the presence of a local angle perception system (i.e. gravity perception is not an exclusive property of the apex) which can produce conditions which interfere with the signal transmission process. Additional signals might be generated, but the signal from the apex could also be affected. If this is true, it is possible to look for a mathematical expression (containing subsection bending speed and its various derivatives) which, plotted against the subsection local angle, produces a single curve. All points for all subsections and at all gravitropic reaction times must lie in this curve.

Using Mathcad, a large number of expressions were tested empirically until it was found that the ratio of local bending rate and the gradient of this local bending rate, plotted against the local angle, produce a single curve (Fig. 10). Hence,

$$\frac{U_\lambda}{U} = \Psi(\alpha_L), \quad (4)$$

where  $U$  is local bending speed,  $U_\lambda$  is its gradient along the stem and  $\Psi(\alpha_L)$  is an empirically determined tangential function of the local angle, valid for all subsections during all times of the gravitropic reaction.

As seen in Figure 10, the angle in the region of 40 to 50° is critical. In this interval  $\Psi(\alpha_L)$  abruptly changes values from large positive to large negative. This interval is similar to the 35°, which was reported as the angle at which curvature compensation begins (Moore *et al.*, 1994). At the moment, it is difficult to suggest what biological features of the system lead to the shape of this function, but this plot clearly supports the hypothesis that the local angle has an important role in signal transmission.

A similar plot was obtained for apex-pinned stems (Figure 11) and contains a critical point in the -65 to -55° region. The points in this plot are dispersed,

indicating that additional factors which are not taken into account by eqn (4), might be affecting the behaviour of apex-pinned stems.

#### *Computer simulation of the gravitropic reaction of the C. cinereus stem*

To determine how well the suggested hypothesis predicts the bending of the stem a program was written which generates a series of images representing a 'theoretical stem' at various stages in its gravitropic response. These images could then be compared with the images of real stems. In writing the program it was supposed that, as for other ordinary and partial differential equations, for sufficiently small steps in time and space the derivative can be approximated by the difference (Collatz, 1966).

To build the program the model equation was rewritten as

$$U = \frac{U_\lambda}{\Psi(\alpha_L)}. \quad (5)$$

The function  $\Psi(\alpha_L)$  was approximated by tangent fit to experimental data. The 'theoretical stem' was divided into 200 subsections, more than was used for digitizing real observations, to produce smoother curvatures. Each subsection had its own local bending speed, and this stored value was used to calculate the gradient for the next iteration.

Using object-oriented programming, the following algorithm was executed simultaneously in all 200 subsections:

1. Find subsection local angle  $\alpha_L$  by integrating curvatures of all subsections below the current with respect to distance from the base.
2. Using approximation of experimentally observed dependence (Fig. 10 or Fig. 11) find  $\Psi(\alpha_L)$  for this subsection.
3. Using information about local bending speed during previous iteration in adjacent subsections find bending speed gradient.
4. From eqn 5, find new local bending rate. It was noticed, that if the step in time is sufficiently small, the values of local bending rate change smoothly from step to step.
5. Change subsection curvature in degree, proportional to calculated bending velocity.
6. Using information about local angles of this subsection and all subsections below find subsection position in space. Display the subsection and go to 1.

#### *Comparison between computer-generated and experimentally observed stem bending*

The first runs immediately indicated, that eqn (4) lacks a signal perception description. This is not surprising, because it was obtained by the methods

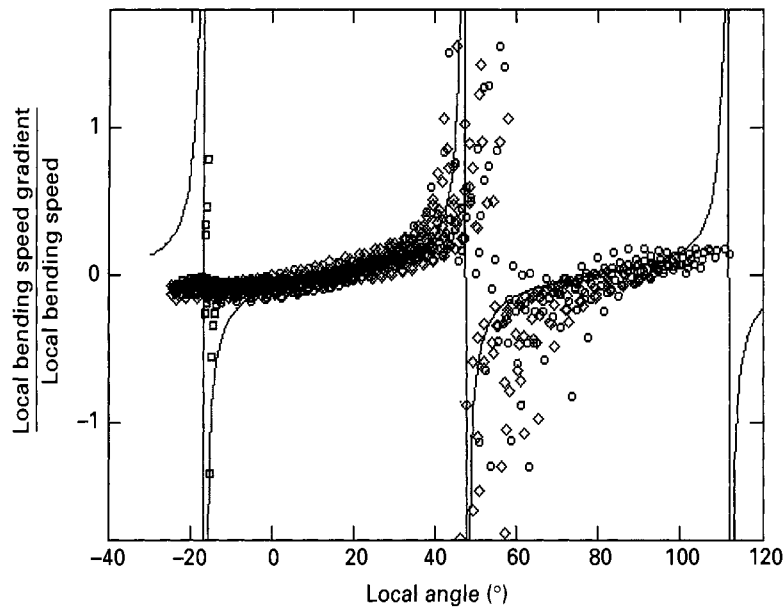


**Figure 10.** Plotting the ratio of change in local bending rate and local bending rate against the local angle for base-pinned *C. cinereus* stems during 400 min of gravitropic reaction.  $\square$ , time before 100 min;  $\diamond$ , time between 110 and 250 min;  $\circ$ , times > 260 min; —, proposed approximation  $\Psi(\alpha_L) = \text{tg}((\alpha_L - 15^\circ) \times 2.8) \times 0.1$ .

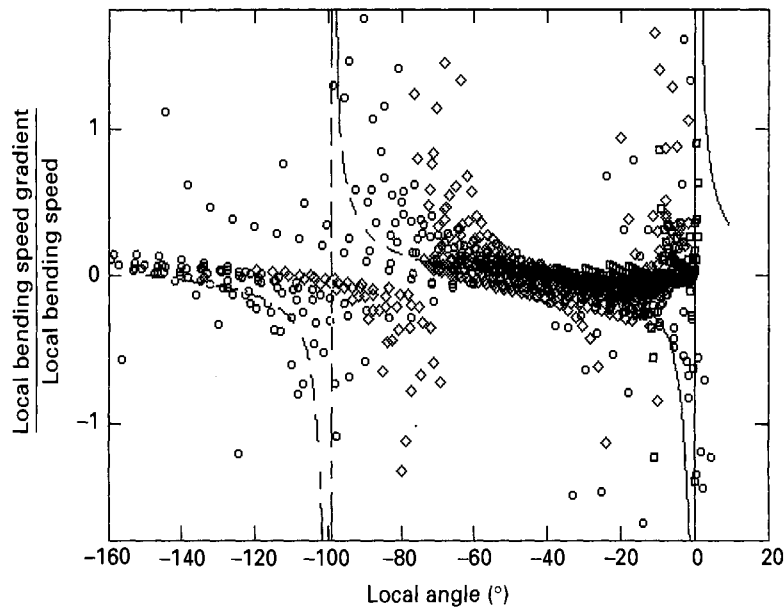


**Figure 11.** Plotting the ratio of the rate of change in local bending rate and local bending rate against the local angle for apex-pinned *C. cinereus* stems during 400 min of gravitropic reaction.  $\square$ , time before 100 min;  $\diamond$ , time between 110 and 250 min;  $\circ$ , times > 260 min; —, proposed approximation  $\Psi(\alpha_L) = \text{tg}(\alpha_L \times 1.8) \times 0.1$ ; ----, area of large angles, where this approximation requires correction.

designed for analysis of signal transmission equations. However, adding a signal source in the apex did not produce a working model. Hence it was necessary to add a signal source distributed along the stem. The biological reality of this suggestion is supported by the ability of *C. cinereus* stems to respond gravitropically with up to 60% of their apical regions removed (Greening *et al.* 1993). The level of this signal was postulated to be proportional to the cosine of the subsection local angle, being maximal in horizontal position ( $\cos 0^\circ = 1$ ) and zero in vertical position ( $\cos 90^\circ = 0$ ). The bending stem shapes produced by this version had much larger curvatures near the base and smaller near the apex than were actually observed. To deal with this it was

supposed that the ability of the stem to perceive the gravitropic signal is highest at the apex and decreases in the basipetal direction. Hence the final model was rewritten as

$$U = \frac{U_\lambda + P(\alpha_L)}{\Psi(\alpha_L)}, \quad (6)$$

where  $P(\alpha_L)$  is a perception function dependent on distance from the apex (which for normalized data is equal to  $1 - \lambda$ ) and local angle:

$$P(\alpha_L) = S_D \cdot \cos(\alpha_L) \cdot e^{-S_D \cdot (1-\lambda)}. \quad (7)$$

The final model, the combination of eqns (6) and (7), accepts two scalar parameters:  $S_D$ , which determines how fast the ability to perceive the gravitropic signal

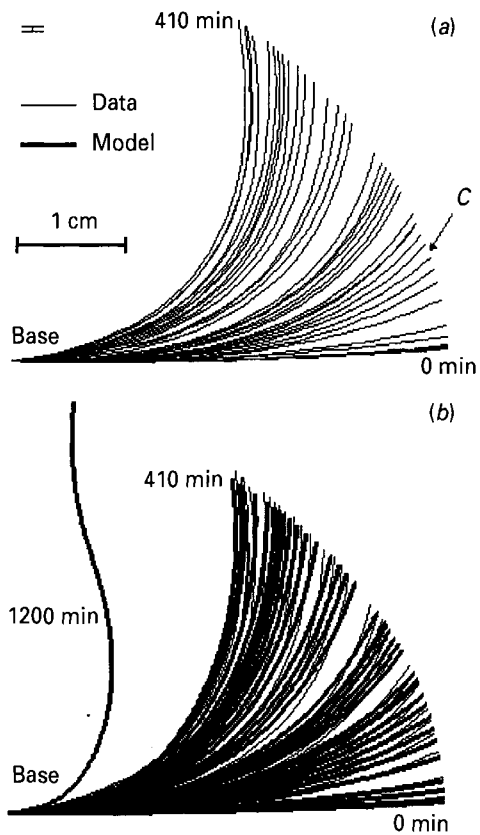


**Figure 12.** Comparison of averaged bending of base-pinned *C. cinereus* stem (a) with (b) the images generated by the model shown as eqn (8) with the perception function shown as eqn (7).  $S_s = 1.45$ ,  $S_D = 15.07$  and  $\Psi(\alpha_L)$  was chosen as best fit to experimental data  $(tg((\alpha_L - 15^\circ) \times 2.8) \times 0.1)$ . In (b), computer-generated images (thick lines) are plotted over the experimentally observed images (regular lines). Times of subsequent images differ by 10 min. (b) also includes a shape, predicted by the model for very late stages (1200 min) of the gravitropic reaction. The error bar defines the maximal SD of mean for experimentally observed shapes. C shows the beginning of the curvature compensation process.

decreases as we move from the apex towards the base, and  $S_s$ , which is more associated with the bending velocity. The approximate values for these parameters are given in the legends of Figures 12 and 13. It also includes one empirically determined function, that takes the angle as its parameter and can be approximated in various ways (the approximation  $\Psi(x) = c_1 tg(c_2 x + c_3)$  was used, see Fig. 10 and Fig. 11). This function determines the perception of the gravitropic signal and the compensation process. By summarizing the equations shown above, we obtain the final equation below ( $t \geq 0$ ;  $0 \geq \lambda \geq 1$ , initial condition  $C_L(0, \lambda) = 0$  (straight stem), boundary conditions  $C_L(t, 0) = C_L(t, 1) = 0$ ).

$$\left(\frac{\partial}{\partial t} C_L(t, \lambda)\right)(t, \lambda) = \frac{\left(\frac{\partial}{\partial \lambda} \left(\frac{\partial}{\partial t} C_L(t, \lambda)\right)(t, \lambda)\right) + S_s \cos\left(\int_0^\lambda C_L(t, l) dl\right) S d e^{(1-\lambda)}}{\Psi\left(\int_0^\lambda C_L(t, l) dl\right)} \quad (8)$$

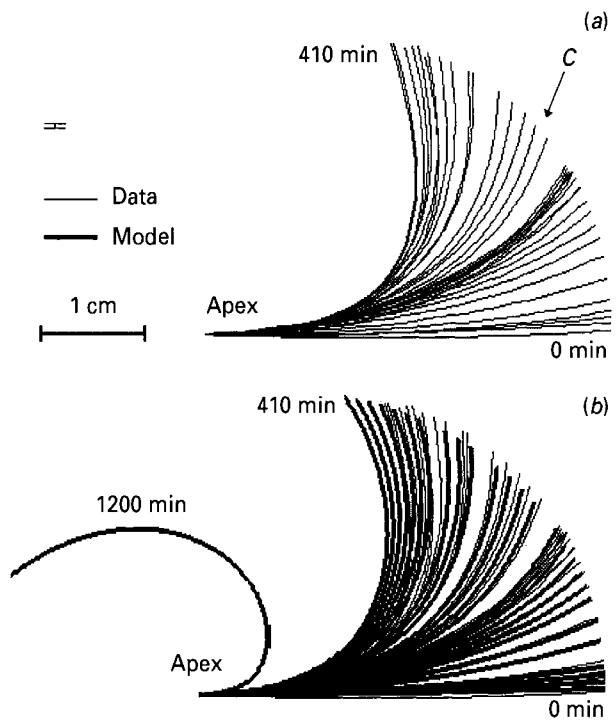


**Figure 13.** Comparison of averaged bending of apex-pinned *C. cinereus* stem (a) with (b) the images generated by the model shown as eqn (8) with the perception function shown as eqn (7).  $S_s = 0.38$ ,  $S_D = 18.24$  and  $\Psi(\alpha_L)$  was chosen as best fit to experimental data  $(tg(\alpha_L \times 1.8) \times 0.1$  if  $\alpha_L > -80$ ;  $0.24$  otherwise). In (b), computer-generated images (thick lines) are plotted over the experimentally observed images (regular lines). Times of subsequent images differ by 10 min. (b) also includes a shape, predicted by the model for very late stages (1200 min) of the gravitropic reaction. The error bar defines the maximal SD of mean for experimentally observed shapes. C shows the beginning of the curvature compensation process.

Using this equation, the program in Pascal was written to obtain numeric solutions.

The shapes generated by the final model for base-pinned stems are shown in Figure 12. This figure also includes the averaged experimentally observed shapes for comparison (rotated to their original position). As can be seen, the model correctly describes the bending process, both early and late stages. A minor deviation can be noticed for intermediate stages (200–300 min), where the model predicts slightly lower curvatures near the middle of the stem. However, the model correctly predicts an S-shaped stem form in very late stages of the gravitropic reaction.

Although no information about the late bending stages was initially included in the model for apex-pinned stems (Fig. 13), the model correctly predicted the late stages of gravitropic reaction as C-shaped (base rotated through over  $180^\circ$ ). In the model, this overshooting is determined by weaker sensitivity of the average value of  $\Psi(\alpha_L)$  to its argument in orientations close to the (inverted) vertical (Fig. 13). Hence in this stage the bending direction and velocity is determined more by the internal system status ('memory') than by changes of stem orien-

**Table 2.** The results of the lack-of-fit test, performed on the final model for both base-pinned and apex-pinned stems

Case	Lack-of-fit mean square	Pure error mean square	°f	Ratio	Value $z$ for which the distribution function $F(z)$ has the value 0.95	Conclusion
Base-pinned stems	$1.1785 \times 10^{-4}$	$4.7028 \times 10^{-4}$	2045, 22550	0.251	Close to 1.000	Differences not significant
Apex-pinned stems	$3.7751 \times 10^{-4}$	$4.8608 \times 10^{-4}$	2045, 24600	0.777	Close to 1.000	Differences not significant

tation. The suggestion can be supported by the argument that turning into inverted vertical position causes bending 'by memory' in plants (Jurkoniene, Maximov & Merkys, 1996; Maximov *et al.* 1996). Whilst points in this extreme interval are comparatively more disperse, the final predicted and observed stem shapes are very similar (Fig. 13). The only noticeable difference is that during intermediate stages of the gravitropic reaction the predicted curvatures near the free base were slightly higher than observed. The validity of the final model was tested with the Lack-of-Fit test (Table 2) which showed predicted curvatures to be not significantly different from reality.

The model successfully generates the main features of the gravitropic bending of base-pinned *C. cinereus* stems. Bending begins near the apex. During the later stages of the reaction the curvature maximum moves in the basipetal direction at decreasing speed until it stops about one third of stem length from the base. The zone from 0.2 to 0.5 of stem length from the base determines the major part of final stem curvature. When the curvature maximum moves from the apex, the apical subsection starts to straighten, performing curvature compensation. In the late stages of the gravitropic reaction the stem becomes S-shaped.

The initial stages of bending of apex-pinned stems seems rather similar, although in this case the response of the fixed apex is stronger. The free basal part after some time also begins to straighten. However, in comparison with base-pinned stem, this reaction is weaker and significantly delayed. After reaching the vertical position base-pinned stems stop bending, whereas apex-pinned stems continue to bend, becoming C-shaped.

Thus, on the one hand it is clear that the stem is polarized: base-pinned and apex-pinned stems bend differently. On the other hand, curvature compensation in the free base of apex-pinned stems may suggest that in earlier stages of evolution the stem was not polarized and that only apex angle, but also the local angle of basal subsections can be important for the gravitropic reaction.

This analysis has indicated that the subsection

local angle most probably affects transmission of the signal through the subsection. If the signal is assumed to be proportional to local bending speed, the ratio of the signal gradient toward the stem and the signal, plotted against the local angle, produces a curve which is the same for all subsections and during all times of gravitropic reaction. It is difficult to suggest any hypothesis about the reasons of such dependence, but it is this which can be substituted into a model which generates bending stem shapes not significantly different from experimental observations. The argument is based on the fact that the points in Figure 10 appear to belong to a single curve. Approximation of this curve enables computed simulation of the bending process. Taking into account two very abrupt changes from large positive to large negative values at approx.  $-20^\circ$  and  $50^\circ$  the general shape of the curve, the function  $y = c_1 \operatorname{tg}(c_2 x + c_3)$  is a good candidate. The  $c_2$  and  $c_3$  parameters can be found from the period and phase required and  $c_1$  can be chosen visually. Subsequently, all three parameters can be optimized using a least-square-fit method (the method of dichotomy was used). It might also be significant that the function  $\operatorname{tg}(x)$  accepts the angle as its argument. In our case the horizontal co-ordinate is also the angle.

In general, therefore, the outcome of this modelling suggests that the gravitropism of the stem of the *Coprinus cinereus* fruit body depends upon:

- production of a bending signal which is transmitted towards the stem base at decreasing speed;
- transmission of the signal through a segment depends on segment orientation, with the most probable basis being that a horizontal segment allows free transmission, a vertical segment permits no transmission;
- the signal can be produced by the apical two thirds of the stem;
- the upper two-thirds of the stem can perceive the gravity vector;
- sensitivity of the gravity vector perception system declines from the apex downwards;

- (f) perception of and reaction to change in the gravity by the basal one-third of the stem is very weak.
- (g) curvature of apical subsections is decreased by curvature compensation which declines in intensity basipetally.

The model is readily adaptable to other circumstances. It is characteristic of *C. cinereus* that the tropic bend involves the major part of the stem. Stems of fruit bodies of *F. velutipes* bend mainly in their apical part (Monzer *et al.* 1994). In terms of this model, it is the apical subsections which mainly define local curvature of the *Flammulina* stem. The basal part remains nearly straight during the whole gravitropic reaction. This kind of gravitropic reaction can be easily simulated by suggesting that the ability of stem segments to perceive gravity decreases in the basipetal direction more rapidly than in *C. cinereus*. To generate curvature distributions characteristic of the stem shapes produced by *F. velutipes* it was only necessary to increase the value of  $C_D$  (which defines the decrement) in the perception function of eqn (7) by about one order of magnitude. The other major difference between *Coprinus* and *Flammulina*, namely the different rate of response, is probably a simple consequence of differences in the extent of the gravitropically active region, which measures a few mm in *Flammulina*, and a few cm in *Coprinus* (Moore *et al.* 1996). Just as the apex angle is a sum of curvatures of all subsections, so the bending rate is a sum of bending rates of all subsections. Hence, increasing the extent of the responding region also increases the rate of the response as measured by the apex angle.

Changing local curvature distribution features in many mathematical models of gravitropic reaction and other plant movements (Johnson & Israelson, 1968; Johnson, 1971; Barlow *et al.*, 1991; Stočkus & Moore, 1996). As a rule, however, this aspect of the models was not compared with experimental data; instead, attention has been restricted to the tip angle. Hence, the method suggested here for establishing curvature distribution directly from experimental data can be usefully applied to further mathematical modelling in this area.

This work examines and successfully models the detailed distributions of local curvature and their changes during tropic curvature for the first time. Significant differences between plant and fungal gravitropic reactions may have emerged. The mushroom stem features a moving maximal curvature point, curvature compensation as a straightening process, and exponentially decreasing ability to perceive the gravitational irritation, all of which might be different than, for example, plant roots. Thorough comparison, however, will require an analogous data set. Hence, the next task will be to apply the method shown here to plant subjects.

## ACKNOWLEDGEMENTS

We thank the British Mycological Society and the Federation of European Microbiological Societies for award of a Fellowship to A.M.

## REFERENCES

- Barlow P, Brain P, Adam J. 1989. Differential growth and plant tropisms: a study assisted by computer simulation. *Environmental and Experimental Botany* **29**: 71–83.
- Barlow P, Brain P, Butler R, Parker J. 1991. Modelling of the growth response of gravireacting roots. *Aspects of Applied Biology* **26**: 221–225.
- Barlow P, Rathfelder E. 1985. Distribution and redistribution of extension growth along vertical and horizontal gravireacting maize roots. *Planta* **165**: 134–141.
- Borwein J, Watters C, Borowski E. *Interactive math dictionary on CD*. Halifax: MathResources Inc.
- Brown A, Chapman D. 1977. Effects of increased gravity force on nutations of sunflower hypocotyls. *Plant Physiology* **59**: 636–640.
- Collatz L. 1996. *The numerical treatment of differential equations. 3rd edn*. New York, NY, USA: Springer-Verlag.
- Evans M, Ishikawa H. 1997. Computer based imaging and analysis of root gravitropism. *Gravitational and Space Biology Bulletin* **10**: 65–73.
- Greening JP, Holden J, Moore D. 1993. Distribution of mechanical stress is not involved in regulating stipe gravitropism in *Coprinus cinereus*. *Mycological Research* **97**: 1001–1004.
- Greening JP, Sánchez C, Moore D. 1997. Coordinated cell elongation alone drives tropic bending in stems of the mushroom fruit body of *Coprinus cinereus*. *Canadian Journal of Botany* **75**: 1174–1181.
- Johnson A. 1971. Geotropic responses in *Helianthus* and their dependence on the auxin ratio – with a refined mathematical description of the course of geotropic movements. *Physiologia Plantarum* **24**: 419–425.
- Johnson A, Israelson D. 1968. Application of a theory for circumnutations to geotropic movements. *Physiologia Plantarum* **21**: 282–291.
- Jurkoniene S, Maximov G, Merkys A. 1996. The model for separated investigation of induction and realization phases of gravitropic reaction. *Russian Journal of Plant Physiology* **43**: 5–9.
- Kher K, Greening JP, Hatton JP, Novak Frazer L, Moore D. 1992. Kinetics and mechanics of stem gravitropism in *Coprinus cinereus*. *Mycological Research* **96**: 817–824.
- Korn RW. 1993. Heterogeneous growth of plant tissues. *Botanical Journal of the Linnean Society* **112**: 351–371.
- Maximov G, Meškauskas A, Jurkoniene S, Merkys A. 1996. The role of calcium in different stages of gravitropic reaction. *Russian Journal of Plant Physiology* **43**: 10–13.
- Merkys A, Laurinavičius R, Jaročius A. 1972. The Cholodny–Went theory and the development of physiology of tropic plant movements. In: *Regulation of Plant Growth and Nutrition. Proceedings of the Symposium Results of investigations of plant Physiology and Biochemistry during 1996–1970*. Minsk, Russia: Science Press (in Russian), 84–95.
- Monzer J, Haindl E, Kern VD, Dressel K. 1994. Gravitropism of basidiomycete *Flammulina velutipes*: morphological and physiological aspects of the graviresponse. *Experimental Mycology* **18**: 7–19.
- Moore D, Greening JP, Hatton JP, Novak Frazer L. 1994. Gravitational biology of mushrooms: a flow-chart approach to characterising processes and mechanisms. *Microgravity Quarterly* **4**: 21–24.
- Moore D, Hock B, Greening JP, Kern VD, Novak Frazer L, Monzer J. 1996. Gravimorphogenesis in agarics. *Mycological Research* **100**: 257–273.
- Moore D, Pukkila P. 1985. *Coprinus cinereus*: an ideal organism for study of developmental biology. *Journal of Biological Education* **19**: 31–40.
- Novak Frazer L, Moore D. 1993. Antagonists and inhibitors of calcium accumulation do not impair gravity perception though

- they adversely affect the gravitropic responses of *Coprinus cinereus* stipes. *Mycological Research* **97**: 113–1118.
- Pankhurst RJ. 1994.** The representation of shape and form by computer. In: Ingram DS, Hudson A, eds. *Shape and Form in Plants and Fungi*. London, UK: Academic Press, 153–168.
- Piskunov N. 1969.** *Differential and integral calculus*. Moscow, Russia: Peace Publishers.
- Prusinkiewicz P, Lindenmayer A. 1996.** *The algorithmic beauty of plants*. New York, NY, USA: Springer-Verlag.
- Rawitscher F. 1932.** *Der Geotropismus der Pflanzen*. Gustav Fisher: Jena.
- Selker J, Sievers A. 1987.** Analysis of extension and curvature during the graviresponse in *Lepidium* roots. *American Journal of Botany* **74**: 1863–1871.
- Silk W. 1989.** On the curving and twining of stems. *Environmental and Experimental Botany*, **29**: 95–109.
- Silk W, Erichson R. 1979.** Kinematics of plant growth. *Journal of Theoretical Biology* **76**: 481–501.
- Stočekus A. 1994.** Basic assumptions and comparison of three gravitropic response models. *Advances in Space Research* **14**: 145–148.
- Stočekus A, Moore D. 1996.** Comparison of plant and fungal gravitropic responses using imitational modelling. *Plant, Cell and Environment* **19**: 787–800.
- Went F. 1928.** Wuchsstoff und Wachstum. *Recueil des Travaux Botaniques Néerlandais* **25**: 1–116.
- Whitham P. 1977.** *Linear and non-linear waves*. New York, NY, USA: John Wiley & Sons.